Adaptation to sine-wave gratings selectively reduces the contrast gain of the adapted stimuli

Debbie Y. Dao
Laboratory of Brain Processes (LOBES), Department of Psychology, USC, Los Angeles, CA, USA

Zhong-Lin Lu
Laboratory of Brain Processes (LOBES), Departments of Psychology and BME, USC, Los Angeles, CA, USA

Barbara A. Dosher
Memory, Attention and Perception (MAP) Laboratory, Department of Cognitive Sciences, UCI, Irvine, CA, USA

Adapting to sinusoidal gratings selectively reduces contrast sensitivity to subsequent test stimuli. To investigate the perceptual processes underlying selective adaptation, we developed an external noise plus adaptation paradigm and a theoretical framework based on a noisy observer model (the contrast-gain-control Perceptual Template Model [cgcPTM]). After adapting to a 45 deg, 2-Hz counter-flickering sine grating of 0.8 contrast, observers performed two-interval forced-choice detection of Gabors of matched spatial frequency, tilted at either 45 or 135 deg and embedded in one of six levels of white external noise (Experiment 1) or embedded in orientation band-pass-filtered external noise (Experiment 2). On the basis of the cgcPTM, we found that adaptation selectively reduced the contrast gain of the perceptual template at the adapted spatial frequency and orientation without altering either pre- or post-gain-control (additive and multiplicative) noises or changing transducer nonlinearity. Modeled as notches on the perceptual templates, the estimated full orientation bandwidth of adaptation at half height was about 8.3 deg.

Keywords: adaptation, contrast-gain control, nonlinear transducer function, bandwidth

Introduction

The ability to adapt to the environment is critical for the survival and evolution of biological organisms. The mammalian visual system has been shown to be highly adaptable (Blakemore & Campbell, 1969a, 1969b; Carandini & Ferster, 1997; Foley & Boynton, 1993; Georgeson & Harris, 1984; Greenlee, Georgeson, Magnussen, & Harris, 1991; Jones & Tulunay-Keesey, 1980; Mather, Verstraten, & Anstis, 1998; Ohzawa, Sclar, & Freeman, 1985; Sanches-Vives, Nowak, & McCormick, 2000b; Shapley & Enroth-Cugell, 1984; Sharpe & Tolhurst, 1973; Tolhurst & Barfield, 1978; Williams, Wilson, & Cowan, 1982). In early stages of processing, the visual system relies on retinal light adaptation to cope with the enormous range of light levels in the environment with a relatively narrow neural dynamic range (Shapley & Enroth-Cugell, 1984). After light adaptation, the absolute level of luminance is relatively unimportant in visual processing. Instead, stimulus contrast or pattern is extracted and becomes more relevant. Whereas much research has demonstrated remarkable contrast/pattern adaptation effects in the visual system, the functional significance of contrast/pattern adaptation is still not entirely clear. Although some have suggested that visual adaptation may improve information transmission in the visual system (Barlow, 1990; Wainwright, 1999), the experimental results have been mixed. Greenlee and Heitger (1988) and Wilson and Humanski (1993) found that prolonged inspection of a high-contrast sine-wave grating reduced the increment thresholds when observers performed contrast discrimination on similar sine-wave gratings with relatively high baseline contrasts. The results have however not been replicated (Foley & Chen, 1997; Ross, Speed, & Morgan, 1993). Previously, Barlow, MacLeod, and van Meeteren (1976) also found no compensatory advantages following adaptation to gratings. In this study, we investigated how grating adaptation alters various components of visual processing using an external noise paradigm in combination with the observer model approach (Ahumada & Watson, 1985; Barlow, 1956; Burgess, Wagner, Jennings, & Barlow, 1981; Lu & Dosher, 1999; Nagaraja, 1964; Pelli, 1981). We discuss the functional implications of these changes following grating adaptation.

Since the original demonstration that prolonged exposure to a sine-wave grating resulted in selective reduction of contrast sensitivity for gratings similar to the adapting stimulus (Blakemore & Campbell, 1969b), the effects of grating adaptation have been investigated in a large number of psychophysical studies. We summarize a few key findings:

1. Reduced contrast sensitivity is observed following adaptation to low-contrast (Tolhurst & Barfield, 1978)

doi: 10.1167/6.7.6 Received February 1, 2006; published June 30, 2006 ISSN 1534-7362

and high-contrast (Blakemore & Campbell, 1969a) adapting gratings in both central and peripheral vision (Greenlee et al., 1991; Sharpe & Tolhurst, 1973; Williams et al., 1982). Maximum contrast sensitivity reduction is found when observers adapt to a high-contrast grating (Foley & Boynton, 1993; Georgeson & Harris, 1984) after which contrast thresholds may be elevated for similar stimuli by up to five times the contrast threshold obtained without adaptation (Blakemore & Campbell, 1969a, 1969b). Adaptation can also reduce the perceived contrast (Hammett, Snowden, & Smith, 1994) and/or size or orientation of similar stimuli (Blakemore & Nachmias, 1971; Pantle & Sekuler, 1968).

2. Contrast sensitivity reduction due to adaptation occurs quickly, requiring exposures to the adapting stimulus as short as 67 ms to elicit a large increase in contrast threshold (Blakemore & Campbell, 1969a; Foley & Boynton, 1993). Despite the quick rise in contrast threshold in the first few milliseconds of adaptation, Magnussen and Greenlee (1985) have reported that thresholds continue to rise for up to 30–60 min of adaptation before saturating. Following exposure to the adaptation stimulus, test contrast threshold elevations are apparent within 50 ms (Foley & Boynton, 1993) to 300 ms (Greenlee et al., 1991) after the termination of the adaptation stimulus.
3. Studies have generally confirmed Blakemore and Campbell's original finding that adaptation effects are specific to the orientation and spatial frequency of the adapting stimulus (Blakemore, Muncey, & Ridley, 1973; Greenlee & Thomas, 1992; Menees, 1998; Stromeyer, Klein, Dawson, & Spillmann, 1982). Orientation bandwidths (width at half height of the orientation tuning curve) of contrast threshold elevation after adaptation have been reported to be between 8 deg (Blakemore & Nachmias, 1971) and 45 deg (Greenlee & Magnussen, 1988). Variations in the estimates between different studies may result from differences in task, stimulus characteristics (Phillips & Wilson, 1984), or both. Spatial frequency bandwidths have been reported to be within one octave of the adapting stimulus spatial frequency (Blakemore & Campbell, 1969b; Stecher, Sigel, & Lange, 1973a, 1973b); beyond one to three octaves of the adapted spatial frequency, facilitation occurs, suggesting channel interdependence (De Valois, 1977; Tolhurst & Barfield, 1978). While adaptation effects are specific to the adapting stimulus in orientation and in spatial frequency, they are independent of grating phase (Foley & Boynton, 1993; Jones & Tulunay-Keesey, 1980).

The cellular mechanisms of grating adaptation have also been extensively studied. Whereas neural activities in lateral geniculate nucleus are not affected by grating adaptation (Derrington & Lennie, 1984; Mafei, Fiorentini, & Bisti, 1973; Ohzawa et al., 1985; but see Solomon, Peirce, Dhruv, & Lennie, 2004), adaptation results in decreased cell responses in cat striate cortex (Dean, 1983; Mafei et al., 1973; Movshon & Lennie, 1979; Ohzawa et al., 1985) and macaque V1 (Sclar, Lennie, & DePriest, 1989); the bandwidth of single-unit adaptation is generally consistent with that of human psychophysics. A relatively clear picture of the effects of grating adaptation in primary visual cortex has recently emerged (Carandini, 2000; Carandini & Ferster, 1997; Sanches-Vives, Nowak, & McCormick, 2000a; Sanches-Vives et al., 2000b): Prolonged exposure to gratings increases membrane conductance and therefore reduces membrane potential of cells in primary visual cortex. Given that GABA antagonists have little effect on adaptation (DeBruyn & Bonds, 1986; McLean & Palmer, 1996), postsynaptic hyperpolarization seems to be the primary cause for the reduced excitability of cortical neurons following adaptation. A more recent study (Crowder et al., 2006) suggests that changes of the intrinsic membrane properties may interact with local intracortical network to produce contrast adaptation.

The cellular contrast response function—spikes per second as a function of stimulus contrast—can be characterized with the Naka–Rushton equation:

$$R = \frac{R_{\max} c^n}{c^n + c_{50}^n} + M, \quad (1)$$

where M is the spontaneous activity level, $R_{\max}$ is the maximum evoked response, c is the contrast of the stimulus, c_{50} denotes the contrast at which the response reaches half its maximum, and n determines the steepness of the response curve. The primary effect of adaptation, then, is to increase c_{50} without changing the slope or maximum evoked response (Carandini & Ferster, 1997; Sanches-Vives et al., 2000b; Sclar et al., 1989; but see Crowder et al., 2006; Finlayson & Cynader, 1995), as in Figure 1.

A number of authors have incorporated cellular mechanisms of grating adaptation into their neural network/mathematical models on adaptation for human observers (Foley & Chen, 1997; Meese & Holmes, 2002; Wilson & Humanski, 1993). Because comparisons of contrast response functions before and after adaptation have provided essential data to elucidate cellular mechanisms of adaptation, these authors have chosen to measure and model effects of adaptation on human increment threshold versus pedestal contrast (TvC) functions.[1] Pedestals are typically sine-wave gratings with similar characteristics as the target grating. In a typical experiment, observers are asked to determine the presence or absence of a target grating superimposed on a pedestal. If one assumes that the limiting noise for contrast discrimination is constant, the TvC functions obtained in pedestal-masking experiments are essentially the derivatives of the pooled contrast response functions of all the cells tuned to the grating stimuli. The derivative was used because it is impossible

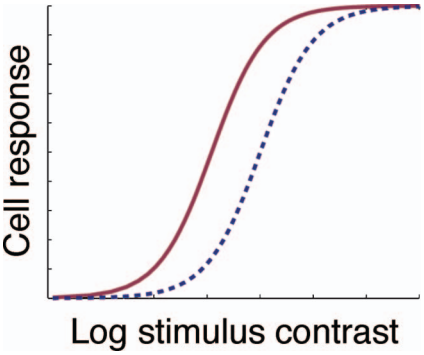

Figure 1. Primary effects of adaptation on cellular contrast response functions. The solid curve represents cell activity (spike rate) as a function of stimulus contrast prior to adaptation; the dashed curve represents cell activity after adaptation. Adaptation shifts the response function to the right without altering its slope and maximum level.

to directly measure contrast response functions over a full contrast range on human observers—observers would be performing at 100% in most detection tasks with moderate stimulus contrasts. Wilson and Humanski (1993) concluded that grating adaptation caused a decrease in the exponent of the power law describing contrast increment thresholds. The empirical basis of their model has since been challenged (Hammett & Snowden, 1995). Foley (1994) and Foley and Chen (1997) have also applied their highly influential pattern-masking model to study the mechanisms of grating adaptation. They concluded that adapting to gratings increased inhibitory interactions in the visual system. We will discuss their model in more detail in the General discussion section.

In this study, we measured and modeled human grating detection thresholds as functions of the magnitude (Experiment 1) and characteristics (Experiment 2) of external noise superimposed on target stimuli with and without adaptation. Compared to pedestal-masking experiments in which adaptation often may have larger or equal impacts on the pedestal than on the target stimulus, the impact of adaptation on white external noise is relatively small. By manipulating the magnitude of external noise, grating detection thresholds vary over a wide range of contrast levels. Therefore, the method offered an alternative way to evaluate the impact of adaptation on contrast response functions. Because the impact of adaptation on white external noise is relatively small, the method essentially provides a direct rather than a derivative evaluation of contrast response function over a full range of contrast levels.

A theoretical framework based on the Perceptual Template Model (PTM; Lu & Dosher, 1999) was used to identify changes in the observer system following adaptation and compare them to cellular mechanisms of adaptation. The PTM approach has been used widely to identify mechanisms of attention (Dosher & Lu, 2000; Lu & Dosher, 1998) and perceptual learning (Dosher & Lu, 1998). To be more consistent with the literature on adaptation, we developed an alternative but mathematically equivalent form of the PTM, the contrast-gain-control PTM (cgcPTM). The cgcPTM was further extended to allow us to estimate the orientation bandwidth of adaptation.

General methods

Apparatus

All stimuli were generated and displayed using MATLAB with the Psychtoolbox extension (Brainard, 1997; Pelli, 1997) on a Macintosh G4 computer. The stimuli were presented on a Nanao Technology FlexScan 6600 monitor with a P4 phosphor and a refresh rate of 120 Hz, driven by the internal video card of the G4. A special circuit (Pelli & Zhang, 1991) that combines two video output channels produced 6,144 distinct gray levels (12.6 bits). A linear lookup table evenly dividing the monitor's entire dynamic range into 256 levels was generated using a psychophysical procedure (Li, Lu, Xu, Jin, & Zhou, 2003). Finer contrast resolution was achieved via linear interpolation. All displays were viewed binocularly with the natural pupil at a viewing distance of 137.5 cm in a dark room with the computer monitor being the only light source.

Stimuli

The adapting stimulus was a sinusoidal grating with spatial frequency equal to 4.0 cycles/deg and tilted +45 deg to the right. It was rendered on a 192 × 192 pixel grid subtending 4.43 × 4.43 deg. The grating was presented in a circular window with a 4.43 deg diameter and was counter-phase flickered at 2 Hz. Counter-phase flickering the adapting stimulus ensured that the mean luminance at any point in space was constant during adaptation; it eliminated afterimages that often appear after adapting to static gratings. To produce the 2-Hz counter-phase flicker, we used 30 image frames for each second that the adapting stimulus was presented. Each frame remained on the screen for four refreshes or 33.3 ms. For each frame n, the luminance $l(x,y)$ at location (x,y) was defined as follows:

$$l(x,y) = l_0\left\{1.0 + c_{\text{peak}}\sin[2\pi f(x\cos\theta - y\sin\theta) + \varphi] \times \sin\left(\frac{2\pi(n-1)}{30}\right)\right\}, \quad (2)$$

where f = 4.0 c/d, $\theta = \pi/4$, l_0 = 27.0 cd/m^2, c_{peak} = 0.80, and $\varphi \in [0,2\pi)$ was a random phase.

The local contrast, $c(x,y) = (l(x,y) - l_0)/l_0$, was therefore:

$$c(x,y) = c_{\text{peak}} \sin[2\pi f(x\cos\theta - y\sin\theta) + \varphi] \times \sin\left(\frac{2\pi(n-1)}{30}\right). \quad (3)$$

The test stimuli were sinusoidal gratings tilted either +45 deg (to the right) or −45 deg (to the left). Each test pattern was rendered on a 64 × 64 pixel grid, subtending 1.48 × 1.48 deg, and presented through a circular window with a 1.48 deg radius. The luminance $l(x,y)$ at location (x,y) was defined as:

$$l(x,y) = l_0\{1.0 + c_{\text{peak}} \sin[2\pi f(x\cos\theta - y\sin\theta)]\}, \quad (4)$$

where f = 4 c/d, $\theta = \pm\pi/4$, l_0 = 27 cd/m^2, and c_{peak} was either determined by a staircase procedure or specified by the experimenter in the method of constant stimuli procedure. The local stimulus contrast was therefore:

$$c(x,y) = c_{\text{peak}} \sin[2\pi f(x\cos\theta - y\sin\theta)]. \quad (5)$$

External noise images of identical size to test stimuli were generated. The details of the external noise images are described in the method section of each experiment.

Design

The effects of adaptation to the test stimuli were measured in a range of external noise conditions. In each external noise condition, two staircases, a 3/1 staircase (three consecutive correct responses resulted in a 10% decrease in signal contrast: $c_{t+1} = 0.90c_t$; one incorrect response resulted in a 10% increase: $c_{t+1} = 1.10c_t$) and a 2/1 staircase (two correct responses decreased signal contrast by 10%: $c_{t+1} = 0.90c_t$; one incorrect response increased it by 10%: $c_{t+1} = 1.10c_t$), were used to determine the contrasts corresponding to 79.3% accuracy ($d' = 1.634$) and 70.7% accuracy ($d' = 1.089$). The trials were randomly interleaved with respect to staircase and external noise conditions.

In addition to the staircase procedure, we also used the method of constant stimuli to assess the impact of adaptation on the full psychometric functions in Experiment 1. In each external noise condition, we sampled the psychometric function at five signal contrast levels (c_1, c_2, c_3, c_4, and c_5) determined from the results of the staircase procedure: $c_2 = c_{70.7\%}$, $c_4 = c_{79.3\%}$, $c_1 = 0.5c_2$, $c_3 = 0.5(c_2 + c_4)$, and $c_5 = 2c_4$. The five signal contrast levels represented an efficient optimal sampling of the psychometric functions (Green, 1990). Again, all trials were randomly interleaved with respect to stimulus contrast and external noise level.

Procedure

A two-interval forced-choice detection task was used in all experiments. Each experimental block began with a 2-min presentation of the adapting +45 deg sine-wave grating, followed by a 1-s presentation of a "blank screen" at the background luminance and then test trials. In the beginning of each test trial, observers were required to readapt to the adapting stimulus for 6 s. They were then presented with two 150-ms test intervals, separated by 500 ms. Each test interval consisted of a brief auditory beep, a 50-ms fixation period, and three images lasting 33.3 ms each. The signal image occurred with equal probability in only one of the two intervals. In the signal-present interval, a "signal" sine-wave grating (+45 deg or −45 deg) was sandwiched by two (independent) external noise images; in the signal-absent interval, a blank image at background luminance was sandwiched by two (independent) external noise images. The observer was asked to identify the interval containing the signal test patch with a key press. A correct response was immediately followed by two brief beeps. A blank screen was displayed to the observer for 1 s before proceeding to the next trial. A typical trial sequence is shown in Figure 2.

Modeling

All the data were fit with the cgcPTM (Appendix A). A least squares procedure was used to fit threshold functions, including the threshold versus external noise contrast functions and the threshold versus external noise orientation bandwidth functions (Hays, 1988). Several variants of the cgcPTM were fit to the data. A gradient-descent method (fminsearch.m, Matlab 7.0) minimized the sum of the squared differences (sqdiff = $[\log(c_{\tau\text{theory}}) - \log(c_\tau)]^2$) between the measured log thresholds and the model-predicted log thresholds. The log approximately equates the standard error over the large range of contrast thresholds, corresponding to weighted least squares, an equivalent to the maximum likelihood solution for continuous data. The goodness of fit for each model was determined by:

$$r^2 = 1.0 - \frac{\sum \text{sqdiff}}{\sum\{\log(c_\tau) - \text{mean}[\log(c_\tau)]\}^2}. \quad (6)$$

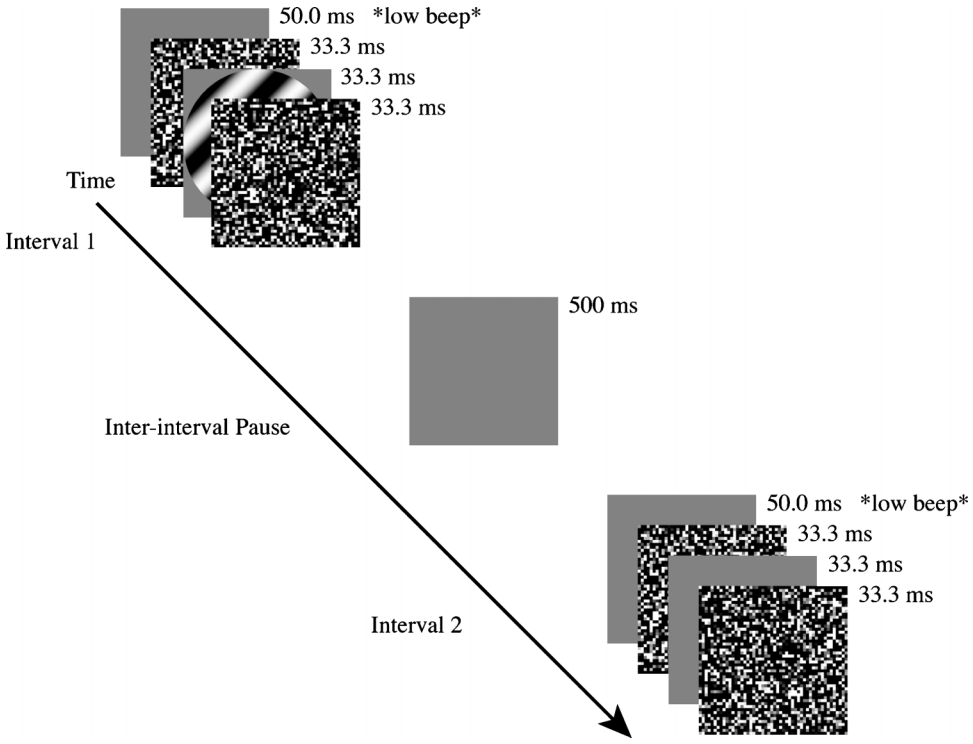

Figure 2. A typical trial with a +45 deg target in the first interval. Each trial began with 6 s of readaptation to the adapting stimulus (not shown).

An F statistic was used to compare nested models:

$$F(df_1, df_2) = \frac{(r^2_{\text{full}} - r^2_{\text{reduced}})/df_1}{(1 - r^2_{\text{full}})/df_2}, \quad (7)$$

where $df_1 = k_{\text{full}} - k_{\text{reduced}}$ and $df_2 = N - k_{\text{full}}$; N is the number of predicted data points.

A maximum likelihood procedure was used to fit psychometric functions in Experiment 1 (Hays, 1988). For each signal contrast and external noise condition i, the probability correct P_{Ci} was computed from either the cgcPTM or Weibull functions. Likelihood is defined as a function of the total number of trials N_i and the number of correct trials K_{Ci} in each stimulus condition i:

$$\text{likelihood} = \prod \frac{N_i!}{K_{Ci}!(N_i - K_{Ci})!} P_{Ci}^{K_{Ci}} (1 - P_{Ci})^{N_i - K_{Ci}}. \quad (8)$$

Again, the Matlab function fminsearch was used to find the best fitting parameters for variants of the Weibull functions or cgcPTM that maximized log(likelihood). Nested models were compared using a χ^2 statistic:

$$\chi^2(df) = 2 \log\left(\frac{\text{max likelihood}_{\text{full}}}{\text{max likelihood}_{\text{reduced}}}\right), \quad (9)$$

where $df = k_{\text{full}} - k_{\text{reduced}}$ is the difference between the number of parameters of the two models.

Experiment 1

The aim of this experiment was to investigate the mechanisms of selective adaptation, that is, the components of the observer system that are affected by selective adaptation. We manipulated the amount of external noise superimposed on the test stimuli to study how selective adaptation affected the TvC functions. Performance was evaluated over a wide range of test contrast levels. Psychometric functions with and without adaptation were compared. The cgcPTM was used to identify the mechanism(s) of selective adaptation.

Methods

We followed the general method described in the General methods section. Some additional information is provided in this section.

External noise images

External noise images were of identical size to the signal images (1.48 × 1.48 deg) and were made of 2 × 2 pixel patches, each subtending 0.065 × 0.065 deg. The contrast

of each pixel patch was sampled from a Gaussian distribution with 0 mean and specified standard deviation contingent upon the desired amount of external noise. Six external noise levels with rms contrasts of 0, 0.0206, 0.0413, 0.0825, 0.1650, and 0.33 were used. The maximum standard deviation of the noise was 0.33. This guaranteed that the external noise conformed to the Gaussian distribution.

Testing conditions

The adapting stimulus was oriented at +45 deg. Across different trials, the test stimuli were oriented at either +45 deg or −45 deg with equal probability. A beep prior to each pair of test intervals indicated to the observer the orientation of the target: A low beep signified a +45 deg target; a high beep signified a −45 deg target. The beeps were used to eliminate target orientation uncertainty.

In the staircase portion of the experiment, threshold contrasts were estimated for both test orientations and all the external noise levels in two 1-hr sessions, with a total of 40 trials per condition for the 3/1 staircase and 32 trials per condition for the 2/1 staircase. The staircases ran continuously across the two sessions.

In the method of constant stimuli portion of the experiment, each observer ran ten 240-trial sessions. There were therefore 40 trials per point on the sampled psychometric function in each test orientation and external noise level condition. A session lasted about 45 min.

In addition, the entire method of constant stimuli procedure was repeated without adaptation to obtain additional "baseline" measures.

Observers

Two University of Southern California students, naive to the study's purposes (A.B. and J.S.), and the first author (D.D.) served as observers in the experiment. All observers had corrected-to-normal vision.

Results

TvC functions from the staircase procedure

Threshold contrasts from the staircase procedure were averaged across observers and are shown in Figure 3 as TvC functions. The shape of the TvC functions was similar to those observed in the literature (Ahumada & Watson, 1985; Barlow, 1956; Burgess et al., 1981; Lu & Dosher, 1999; Nagaraja, 1964; Pelli, 1981). Threshold contrasts in the adapted orientation (+45 deg) are significantly higher than those in the unadapted orientation (−45 deg). At the criterion performance of 79.3% correct measure (3/1 staircase), adaptation increased the average threshold by 111.6% in the three lowest external noise contrast conditions and 77.9% in the three highest external noise conditions. At 70.7% correct (2/1 staircase), adaptation increased the average threshold contrast in the low-noise conditions by 117.8% and that in the high-noise conditions by 60.0%.

The threshold ratio between these two criterion performance levels was 1.31 ± 0.05 in the unadapted orientation; it was 1.35 ± 0.05 in the adapted orientation. The ratio was not altered by adaptation. This ratio invariance implies that the nonlinear transducer and contrast-gain-control components of the observer model were not affected by adaptation (Lu & Dosher, 1999).

In summary, adaptation increased thresholds throughout all the external noise levels. The magnitude of threshold elevation was higher in low external noise than in high external noise. We suggest that the different magnitude of adaptation effects in low and high external noise conditions is due to effects of adaptation on external noise. Similar magnitudes of adaptation were found at both criterion levels, suggesting that adaptation does not result from changes in nonlinear transducer or contrast-gain control.

Psychometric functions

For each observer, four psychometric functions were obtained in each of the six external noise conditions, including a psychometric function for the test stimuli in the adapted orientation, test stimuli orthogonal to the adapted orientation, and the two psychometric functions in the no-adaptation sessions. All these psychometric functions were fit with the Weibull function:

$$P = 0.50 + (\max - 0.50)\left(1 - 2^{-(c/\alpha)^{\eta}}\right), \qquad (10)$$

where P is the proportion correct, max (<1.0) is the maximum proportion correct, c is the contrast of the test stimulus, α represents the horizontal shift of the function, and η is the slope of the function. A maximum likelihood procedure was used to fit the curves (see General methods section).

Our informal observation suggested that (1) three of the four experimental conditions, detection of a −45 deg grating following adaptation to the +45 deg grating and detection of either a +45 deg or a −45 deg grating without adaptation, generated equivalent data and (2) the difference between the three "control" conditions and the adapted condition was only a change in the horizontal shift of the psychometric functions; the slope remained unchanged. We therefore conducted nested model tests to verify these observations.

A model lattice was constructed for each external noise condition. Each lattice consisted of nine separate models. In the fullest model (the $4\alpha 4\eta 4$max model), there are 4 α values, 4 η values, and 4 max values, for a total of 12 parameters. In the most reduced model ($1\alpha 1\eta 1$max), no parameters were free to vary among the conditions. Of particular interest to us was a $2\alpha 1\eta 1$max model that had one independent α for test stimuli in the adapted orientation following adaptation and another independent

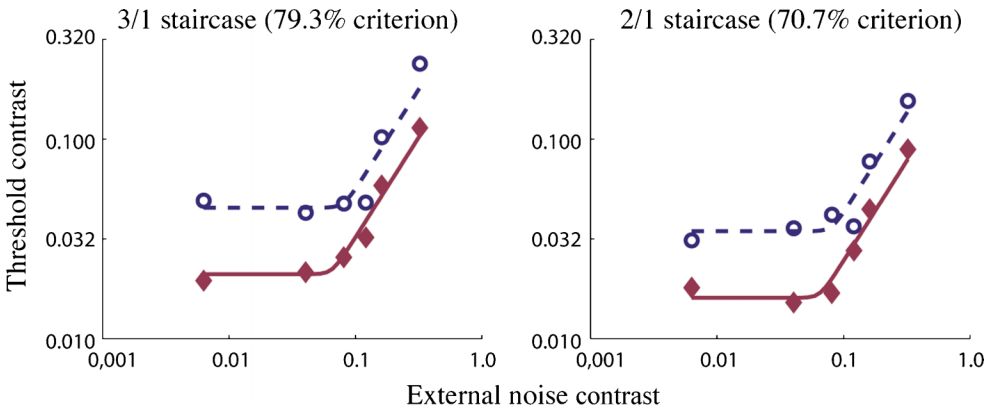

Figure 3. Average threshold versus contrast functions for data collected using the staircase. The data on the left panel are from the 3/1 staircase; those on the right are from the 2/1 staircase. There is an increase in contrast threshold at all external noise and both criterion levels following adaptation. Smooth curves represent the predictions of the best fitting cgcPTM. Control (no adaptation) conditions are represented by solid lines and diamonds (-♦-); the adapted condition is represented by dashed lines and circles (-○-).

α for all the other three control conditions but the same η and max across all the four conditions.

For all observers and in all noise levels, the $2\alpha1\eta1$max model described in the previous paragraph provided the most parsimonious fit to the data (r^2 = .88 ± .06, .88 ± .04, and .88 ± .07 for A.B., D.D., and J.S., respectively). The quality of the fit from this reduced model is statistically equivalent with the fullest $4\alpha4\eta4$max model ($p > .10$). In all but two cases, this $2\alpha1\eta1$max model is significantly better ($p < .005$) than the $1\alpha1\eta1$max, which assumes no adaptation effect. In those two cases, the $2\alpha1\eta1$max model provided marginally better fits than the $1\alpha1\eta1$max ($p < .06$). The measured psychometric functions and their best Weibull fits are shown in Figure 4, where the three control conditions have been pooled and shown as a single function. We used the pooled data in subsequent analyses.

In summary, we found that the three control conditions, detection of a −45 deg grating following adaptation to the +45 deg grating, detection of either a +45 deg or a −45 deg grating without adaptation, generated equivalent data. Adaptation shifted the corresponding psychometric functions horizontally without altering their slopes. This is consistent with the effect of adaptation on cellular contrast response functions (Carandini & Ferster, 1997; Sanches-Vives et al., 2000b; Sclar et al., 1989).

TvC functions from the method of constant stimuli procedure

Threshold contrasts at 65%, 75%, and 85% correct were derived from the Weibull fits to the psychometric functions. The thresholds are plotted as TvC functions in Figure 5 for the average observer.

The TvC functions show the same pattern observed in the staircase data. There is an increase in threshold contrast in the adapted condition when compared to the control conditions. Again, there is a higher threshold increase at lower external noise levels than at higher external noise levels. In the three lowest external noise conditions, there were average increases of 98.0%, 98.5%, and 98.9% in threshold contrast in the 65%, 75%, and 85% criterion levels, respectively. In the three highest external noise conditions, there were average increases of 81.7%, 82.3%, and 82.6% in threshold contrast in the 65%, 75%, and 85% criterion levels, respectively.

The threshold ratio between 75% correct and 65% correct was 1.27 ± 0.09 in the control conditions and 1.27 ± 0.09 in the adapted orientation. The threshold ratio between 85% correct and 75% correct was 1.23 ± 0.07 in the control conditions and 1.23 ± 0.07 in the adapted orientation. The ratios did not change following adaptation. The ratio invariance between the adapted and unadapted conditions implies that the nonlinear transducer and contrast-gain-control components of the observer model were not affected by adaptation (Lu & Dosher, 1999).

Modeling: TvC functions

The PTM (Lu & Dosher, 1999) was proposed to explicitly model nonlinear psychometric functions (Pelli, 1985) and the Weber law behavior of the perceptual system (Burgess & Colborne, 1988). The original PTM includes a nonlinear transducer function and a form of multiplicative noise to account for the nonlinear properties in perception. However, contrast-gain-control rather than multiplicative noise is a more familiar model construct in the neurophysiology literature (e.g., Heeger, 1993). In Appendix A, we developed a contrast-gain-control variant of the PTM (cgcPTM) and showed that it is mathematically equivalent to the original PTM at the level of d' prediction. The cgcPTM (Figure A1) consists of six elements: (1) a perceptual template with gain β, (2) a nonlinear transducer function with exponent γ, (3) pre-gain-control internal noise N_1, (4) divisive contrast-gain control, (5) post-gain-control internal noise N_2, and (6) a

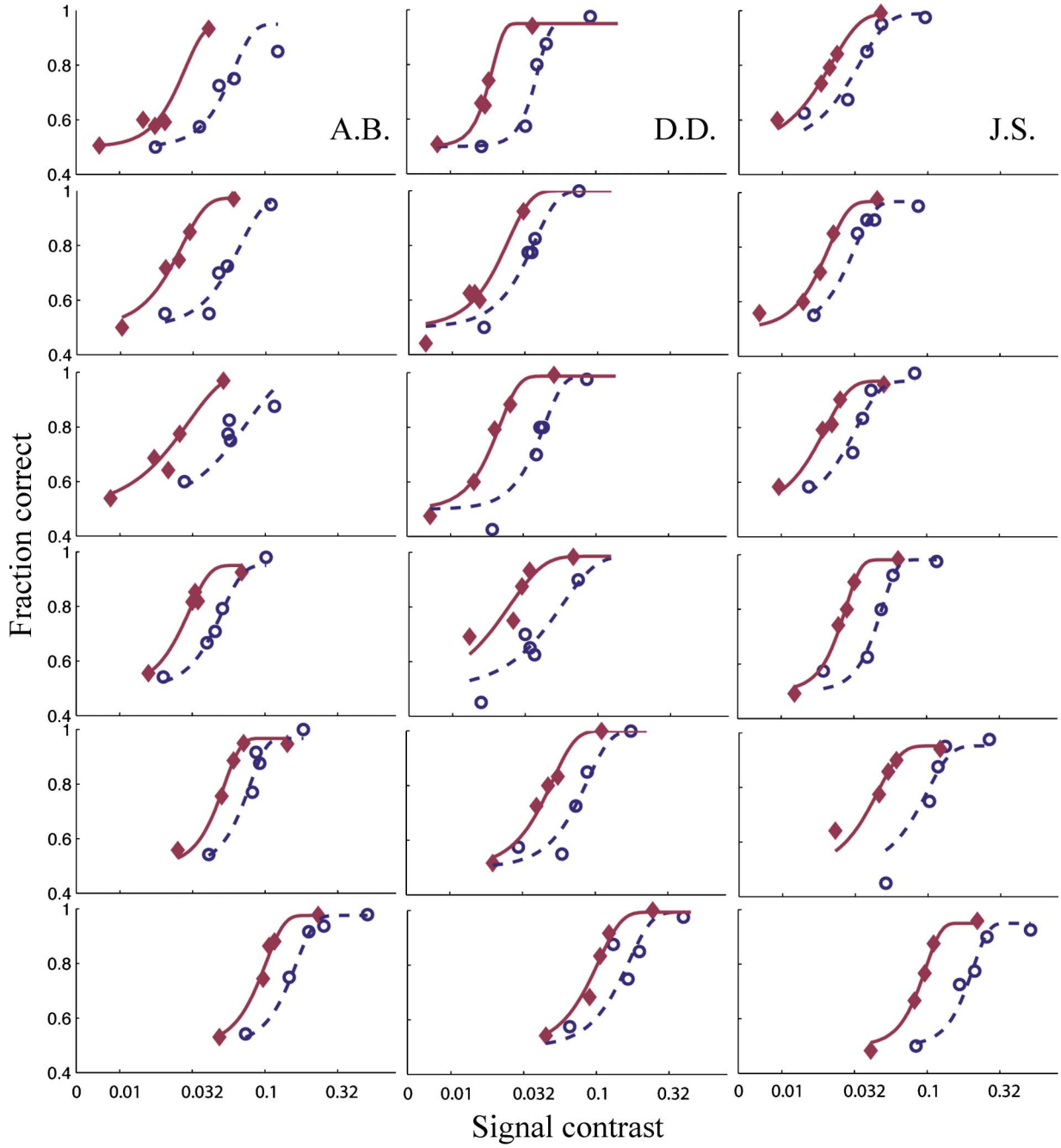

Figure 4. Psychometric functions for the three observers (from left to right) in six external noise conditions (from top to bottom), fit with Weibull functions. The adapted condition is represented by dashed lines and circles (-○-); control conditions are represented by solid lines and diamonds (-◆-).

decision process. Within the cgcPTM framework, we can test effects of adaptation on various combinations of the following potential mechanisms (see Appendix A for details): (1) reducing the contrast gain to signal stimuli, (2) reducing the contrast gain to external noise, (3) altering the exponent of the nonlinear transducer function, (4) changing the magnitude of pre-gain-control internal noise, and (5) changing the magnitude of the post-gain-control internal noise.

The full model lattice consisted of 32 different combinations of all the possible mechanisms of adaptation. In the fullest model (Model 1), adaptation was postulated to have resulted in all the possible changes in the observer model. We focused on the six most meaningful reduced models in addition to the fullest model. In Model 2, adaptation only affects both the pre- and post-gain-control internal noises. In Model 3, adaptation reduces the gains to signal and external noise. In Model 4, adaptation only changes the

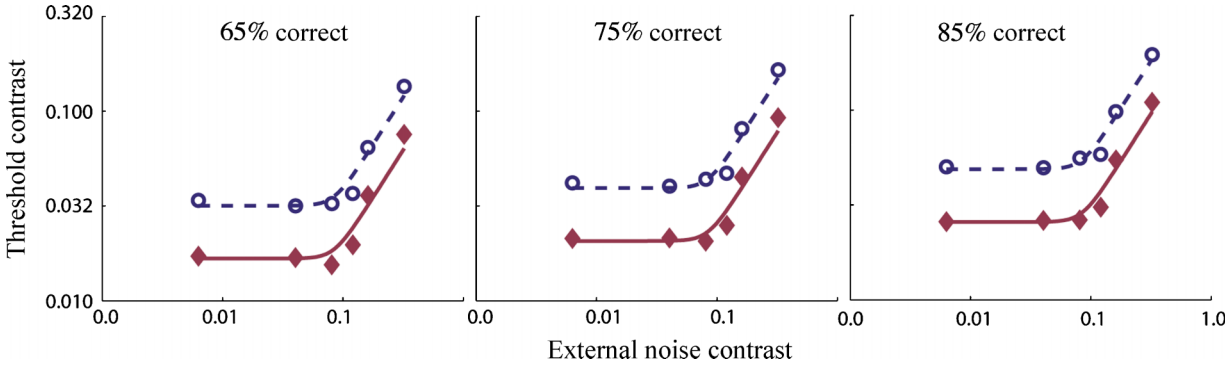

Figure 5. Threshold versus contrast functions at three threshold criterion levels averaged across observers. The adapted condition is represented by dashed lines and circles (-○-). Control conditions are represented by solid lines and diamonds (-♦-).

exponent of the nonlinear transducer. In Model 5, adaptation only impacts the gain to signal stimuli. In Model 6, adaptation only impacts the gain to external noise. Lastly, in the most reduced model (Model 7), adaptation has no impact on any of the components of the observer model.

We first fit the models to the average data from the staircase method. We found that both Model 3 and Model 5 produced statistically equivalent fits to the data when compared with the full model, $F(3,16) = 0$, $F(4,16) = 0.4009$ (both $p > .80$), whereas all the other models produced inferior fits to the data ($p < .001$). Although the fits of Models 3 and 5 are statistically equivalent, $F(1,19) = 1.1190$ ($p > .25$), Model 3 is more appropriate because adaptation in principle should have affected the gain to both the signal and the external noise; in addition, it also allows us to capture the smaller magnitude of adaptation effect in the observed high external noise conditions. The model is also statistically superior to all its other reduced models ($p < .001$). For the average observer, Model 3 accounts for 95.4% of the variance with the following parameters: $N_1 = .0046$, $N_2 = .5105$, $b = .001$, $\beta = \beta_2 = 4.645$, $\gamma = 3.0$, $u_1 = .4679$, and $u_2 = .8133$. In other words, the gain to the signal stimuli was reduced by about half and the gain to external noise was reduced by about 19%.

We also fit the TvC functions from the method of constant stimuli. A similar model selection was obtained when we fit the TvC functions derived from the fitted Weibull functions at 65%, 75%, and 85% correct. The best fitting model accounted for 97.4% of the variance with the following parameters: $N_1 = .0060$, $N_2 = .3276$, $b = .001$, $\beta = \beta_2 = 4.641$, $\gamma = 3.0$, $u_1 = .5185$, and $u_2 = .9248$. As with the staircase data, the stimulus gain was reduced by about 50%. The gain on external noise was reduced by about 8%.

Modeling: Full psychometric functions

Psychometric functions for individual observers were fit directly with Model 3 using the maximum likelihood procedure. The results are shown in Figure 6.

The model provided reasonably good fits to the data. r^2 was .87 ± .02, .80 ± .04, and .80 ± .04 for A.B., D.D., and J.S., respectively. The best fitting model parameters are listed in Table 1. The model parameters are in general agreement with those obtained from modeling the corresponding TvC functions.

Summary and discussion

In Experiment 1, we measured the impact of grating adaptation on grating detection in a full range of white external noise conditions. We found that adaptation increased detection threshold across all the external noise conditions, with a slightly larger impact in low than in high external noise conditions. At each external noise level, the magnitude of threshold increase did not depend on the performance criterion used to define the threshold; adaptation simply shifted the psychometric function to the right without changing its slope (in log). On the basis of the cgcPTM, we concluded that adaptation (1) reduced the contrast gain to stimuli similar to the adapting stimuli, including the testing grating at +45 deg and the external noise components that are similar to the adapting stimuli, and (2) did not change the nonlinear transducer or contrast-gain control in the perceptual system. These

Observer	N_1	N_2	b	β, β_2	γ	u_1	u_2
A.B.	.0030	.3031	.0001	4.768	3.000	.3711	.9891
D.D.	.0025	.2526	.0001	4.966	2.989	.5231	1.000
J.S.	.0032	.2910	.0001	5.472	2.527	.5495	1.000

Table 1. Best fitting cgcPTM parameters to the psychometric functions.

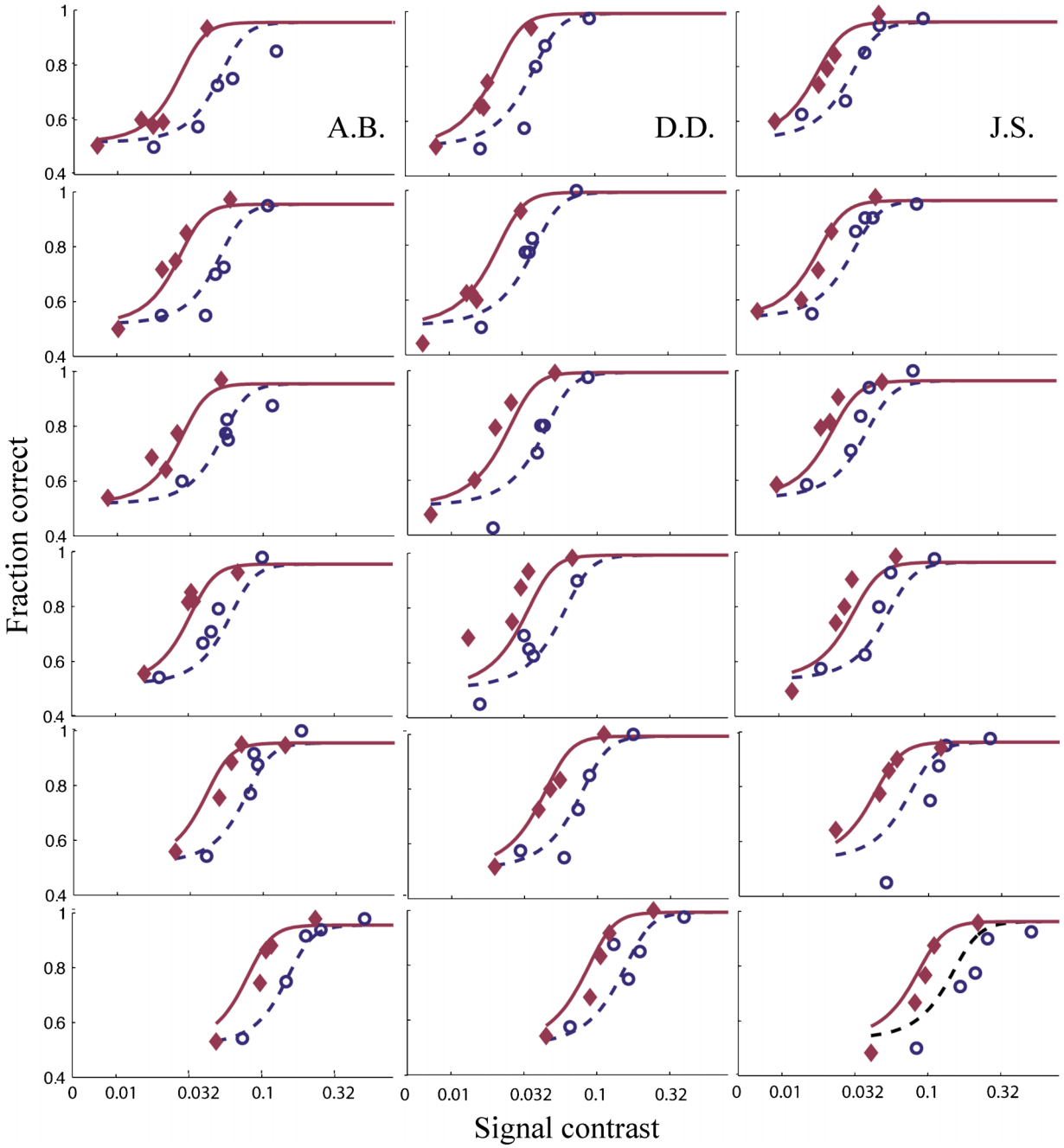

Figure 6. cgcPTM fits of the psychometric functions in the adapted (dotted lines) and control conditions (solid lines).

results are compatible with the findings in neurophysiology (Carandini & Ferster, 1997; Sanches-Vives et al., 2000b; Sclar et al., 1989).

Experiment 2

In Experiment 1, we investigated the impact of adaptation on full psychometric functions and thresholds at multiple performance levels across a wide range of external noise conditions. The results suggested that adapting to a grating stimulus selectively reduces the contrast gain to a narrow range of the stimulus domain. In this experiment, we empirically tested this prediction by directly measuring the orientation bandwidth of adaptation. Observers were adapted to a grating of +45 deg, and then detected the presence of a +45 deg grating in a 2IFC procedure in the presence of external noise with different orientation bandwidths. Nine different noise bandwidths were tested: ±0, 1, 5, 10, 15, 30, 45, 60, and 90 deg about the center orientation of +45 deg. The rich data set also provided enough constraints for us to separately estimate the shape of perceptual template in the signal and the contrast-gain-control paths of the

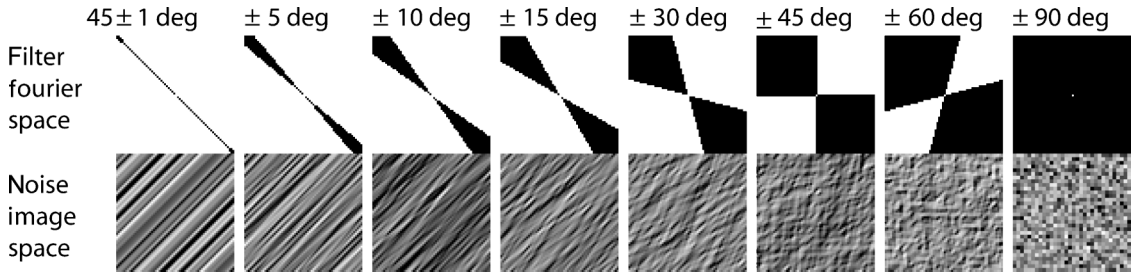

Figure 7. Filtered external noise stimuli in Fourier and real space.

cgcPTM before and after adaptation. We evaluated the orientation bandwidth of grating adaptation.

Methods

Stimuli

Nine orientation-filtered external noise conditions were used. External noise frames were of identical size to signal frames and were made of 2 × 2 pixel patches, each subtending 0.065 × 0.065 deg. The following procedure was used to generate the external noise frames: First, the contrast level of each pixel patch was sampled from a Gaussian distribution with 0 mean and 0.33 standard deviation. Next, the noise image was filtered in Fourier space with filters centered at 45 deg with orientation bandwidths of ±0, 1, 5, 10, 15, 30, 45, 60, and 90 deg. The inverse Fourier transformations of the filtered external noise images were presented as external noise stimuli. There were nine noise orientation bandwidth conditions. The filters and examples of the filtered external noise are shown in Figure 7.

Control conditions

Prior to each adaptation session, observers ran a 2IFC grating detection task without adaptation. This served as a control for measuring detection thresholds prior to adaptation.

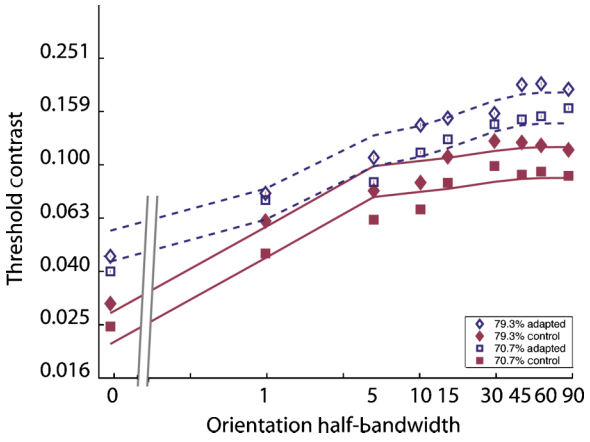

Figure 8. Threshold contrasts as functions of the orientation half bandwidth of external noise. Smooth curves depict the predictions of the best fitting cgcPTM (dotted lines: adapted; solid lines: control).

Observers

One University of Southern California student, naive to the study's purposes (C.C.), and the first author (D.D.) served as observers in the experiment. Both observers had corrected-to-normal vision.

Results

Empirical

The average contrast thresholds for the two observers are plotted in Figure 8 as functions of the bandwidth of external noise. The data are organized by staircase and adaptation conditions.

In all conditions, contrast thresholds increased as functions of the orientation half bandwidth of external noise when $\Delta\theta < 30$ deg and leveled off when $\Delta\theta \geq 30$ deg. Following adaptation, there was a general increase in threshold contrast in all external noise conditions in both staircases: 52.6% in the 2/1 staircases and 58.2% in the 3/1 staircases. The average threshold ratio between the 3/1 and 2/1 staircases was 1.27 ± 0.02 in the unadapted condition and 1.21 ± 0.03 in the adapted condition. Again, adaptation did not change the threshold ratios. This ratio invariance implies that the nonlinear transducer and contrast-gain-control components of the observer model were not affected by adaptation (Lu & Dosher, 1999).

Modeling

Intuitively, the bandwidth of a (symmetric) template can be estimated from the sensitivity to external noise with various orientation bandwidths. If increasing the orientation range of external noise has little effect on performance, then that region is outside the template. To provide a quantitative estimate of the bandwidth of the perceptual template, we extended the cgcPTM in Appendix B. In this extension, the shapes of the perceptual templates in the signal and the gain-control paths of the model were assumed to be Gaussians centered at 45 deg. The two templates could differ—the standard deviations of the two Gaussian-shaped templates were σ_1 and σ_2. On the basis of the results of Experiment 1, we modeled the impact of adaptation as "notches" on the perceptual templates in the

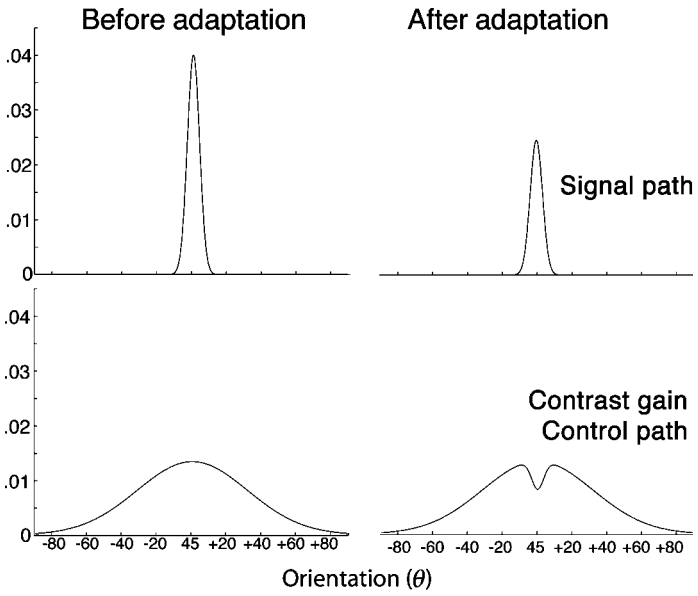

Figure 9. Model results in Experiment 2: perceptual templates before and after adaptation.

signal and the gain-control paths. In the model presented in Appendix B, the notch is assumed to be Gaussian shaped, with standard deviation σ_3. We have also constrained the relative amplitude of the notch in the signal and the gain-control paths to be proportional to the height of the corresponding templates at 45 deg (Equations B3 and B4), and therefore, only the amplitude of one of the notches was free to vary. We have also tested another form of the model in which both the shapes and the amplitudes of the notch in the signal and gain-control paths were free to vary. The model provided only marginally better fit to the data, $F(2,24) = 3.165$, $p = .06$.

From the best fitting model, the template in the signal path is estimated to be narrower ($\sigma_1 = 3.51$ deg, full bandwidth at half height [FBHH] = 8.28 deg) than that in the contrast-gain-control path ($\sigma_2 = 31.7$ deg, FBHH = 74.6 deg) prior to adaptation. Adaptation was measured as a notch on each of the two perceptual templates. The notch had an FBHH of 8.26 deg with an amplitude of $k_3 = 0.3857$. The model accounted for 95.6% of the variance in the data. The other parameters of the model are as follows: $N_1 = .0085$, $N_2 = .7998$, $b = .001$, $\beta = 4.721$, $\beta_2 = 0.5665$, $\gamma = 1.495$, and $u_1 = .4838$. The templates before and after adaptation are depicted in Figure 9.

Summary

In this experiment, observers were adapted to a grating at +45 deg and then detected the presence of a +45 deg grating in a 2IFC procedure in the presence of external noise with a range of orientation bandwidths. Compared to performance in unadapted control conditions, adaptation led to a general elevation in threshold in all noise conditions, with greater threshold elevation in the no-noise condition (0 bandwidth). A cgcPTM with template notches caused by adaptation well accounted for all of the data. The bandwidth of adaptation, defined as the full bandwidth of the "notch" produced by adaptation at half height, was about 8.26 deg.

General discussion

In Experiment 1, full psychometric functions were measured for a detection task in four conditions. In the adapted condition, observers adapted to and detected a grating oriented at +45 deg. In the first control condition, observers adapted to a grating oriented at +45 deg and detected a grating oriented at −45 deg. The remaining control conditions involved detection of a grating oriented at either +45 deg or −45 deg without adaptation. Data for each condition were collected in six external noise levels; five different test contrasts were used to measure each psychometric function. As expected, following adaptation to a grating of a specific orientation and spatial frequency, observers' detection threshold contrasts were increased for stimuli of the same orientation and spatial frequency. An increase in threshold was not observed in the orthogonal orientation; in fact, all of the control conditions generated equivalent data. In agreement with previous observations (Snowden & Hammett, 1996; Stromeyer, Klein, & Sternheim, 1977), adaptation produced a rightward shift in the psychometric functions without any slope change.

Our analysis of the data suggested that the effects of adaptation did not reflect a change in nonlinear transducer or contrast-gain-control. This was substantiated by the fact that threshold increases were consistent across criterion levels and by testing and validating the best fitting cgcPTM model. Foley (1994) and Meese and Holmes (2002) have also presented models in which nonlinearity is unaltered by adaptation. The cgcPTM model analysis suggests that adaptation results in diminished contrast gain to the adapted channel.

Our conclusion is compatible with the observed cellular mechanisms of adaptation in the primary visual cortex of cat (Carandini & Ferster, 1997; Ohzawa et al., 1985; Sanches-Vives et al., 2000a, 2000b) and monkey (Gardner et al., 2005; Sclar et al., 1989). For single cells, adaptation results in a rightward shift of cellular contrast response functions without any slope changes, whereas at the behavioral level, there was a lateral shift in psychometric functions. Data at both levels implicate reduced contrast gain to the adapted stimulus. At the neural level, the work of Sanchez-Vives et al. strongly suggests that postsynaptic hyperpolarization is responsible for decreased cellular activity following adaptation—not changes in presynaptic processes. These and our observation that adaptation did not alter nonlinear transducer and gain control are also consistent with the finding that adaptation does not alter (presynaptic) inhibitory inputs to the cells (DeBruyn & Bonds, 1986; McLean & Palmer, 1996)—changes of

inhibitory inputs to the cells would have resulted in changes of the slope of the psychometric functions. Because there are parallel changes in activity at the neural and behavioral levels, it is possible that the effects of postsynaptic changes might be generalized to describe changes at the behavioral level.

Our results are also consistent with a recent fMRI study (Gardner et al., 2005). Using an event-related design, Gardner et al. found that BOLD contrast response functions in V1, V2, and V3 shifted to approximately center on the adapting contrast. Interestingly, these authors also found that human V4 responded positively to contrast changes, independent of the sign of the changes, suggesting that V4 might not respond to contrast per se but rather to stimulus salience (Lu & Sperling, 1995).

Several computational models based on contrast-gain control have been proposed to account for the effects of adaptation at the behavioral level (Foley, 1994; Georgeson & Harris, 1984; Meese & Holmes, 2002; Wilson & Humanski, 1993). Wilson and Humanski (1993) developed a divisive feedback gain-control model in which a stimulus passes through (1) oriented receptive fields, (2) response nonlinearity, and (3) gain-control units. Each gain-control unit receives a weighted sum of output responses from multiple channels. The gain-control unit then provides divisive feedback to adjust the gain of the receptive fields. Adapted channels are hypothesized to have strengthened connections between the summation process and the gain-control unit, thereby receiving increased inhibitory feedback from their gain-control units and displaying decreased activity. The Wilson–Humanski model was primarily motivated by two empirical observations: (1) grating adaptation produced no threshold elevation at a 30-ms test duration but a normal threshold elevation at 500 ms (Wilson & Humanski, 1993), suggesting adaptation affects the feedback system, and (2) grating adaptation caused a decrease in the exponent of the power law describing contrast increment thresholds (Greenlee & Heitger, 1988; Wilson & Humanski, 1993). These empirical observations have since been challenged. Hammett and Snowden (1995) found that grating adaptation yielded threshold elevation for briefly presented stimuli and that threshold elevation is greater for high than low temporal frequency adapting patterns. Foley and Chen (1997) and Ross et al. (1993) found that prolonged inspection of a high-contrast sine-wave grating did not change incremental thresholds when observers performed contrast discrimination on similar sine-wave gratings with relatively high baseline contrasts (Foley & Chen, 1997; Ross et al., 1993). It is still unclear why different researchers obtained rather different results (Foley & Chen, 1997; Ross et al., 1993), but it is clear that some of these results are inconsistent with the predictions of the Wilson–Humanski model. In addition, the notion that adaptation strengthens inhibition seems to be at odds with the physiology finding that adaptation does not alter (presynaptic) inhibitory inputs to the cells (DeBruyn & Bonds, 1986; McLean & Palmer, 1996).

Foley (1994) and Foley and Chen (1997) have also applied their highly influential pattern-masking model to study the mechanisms of grating adaptation. The model's response is described by an elegant equation:

$$R = \frac{\max\left(0, \sum_{ij} c_{ij} S_{\mathrm{E}ij}\right)^{p}}{\sum_{j}\left(\sum_{i} c_{ij} S_{\mathrm{I}ij}\right)^{q} + Z}, \tag{11}$$

where i and j are index orientation and spatial frequency, respectively; c_{ij} denotes the contrast of grating ij; $S_{\mathrm{E}ij}$ and $S_{\mathrm{I}ij}$ denote the excitatory and inhibitory sensitivities of the pattern detector to grating ij, respectively; p and q are exponents of the nonlinear transducer functions in the excitatory and inhibitory pathways, respectively; and Z is a constant that is stimulus independent. In this model, the inhibitory terms corresponding to the same orientation i are summed prior to being raised to power q. Measuring TvC functions with vertical and horizontal grating masks for a vertical target with and without adaptation to vertical, horizontal, and plaid patterns. Foley and Chen (1997) concluded that adapting to vertical gratings and plaids increased Z and the inhibitory sensitivity to horizontal gratings $S_{\text{I-hor}}$; adapting to horizontal gratings decreased $S_{\text{I-hor}}$. The increase of both Z and $S_{\text{I-hor}}$ following adaptation to vertical gratings is mathematically equivalent to decreases of excitatory and inhibitory sensitivities to vertical gratings. Reformulating the Foley–Chen model of adaptation, we found that it is mathematically equivalent to another model in which adapting to horizontal gratings only affected the sensitivity to horizontal gratings. Moreover, the reformulated Foley–Chen account of adaptation would be more consistent with cellular mechanisms of adaptation, as well as with the conclusions of this study.

Although the functional forms of the cgcPTM and the Foley model seem to be similar, they are developed in rather different experimental domains—the domain of external noise masking is very different from that of pedestal masking. Compared to pedestal-masking experiments in which adaptation often may have larger or equal impacts on the pedestal than the target stimulus, the impact of adaptation on white external noise was relatively small. By manipulating the magnitude of external noise, grating detection thresholds vary over a wide range of contrast levels. Therefore, the external noise method offered an alternative way to evaluate the impact of adaptation on contrast response functions. Decreased contrast sensitivity appears to be the result of a decrease in contrast gain to the adapted stimulus at and around the adapted orientation. Testing at a full range of contrast values, we find similar changes in response at the observer level as has been

reported at the cellular level. In Experiment 2, we elaborated our empirical method and the cgcPTM model to estimate the bandwidth of adaptation. An FBHH of 8.26 deg was obtained. The bandwidth is very similar to the 8 deg reported by Blakemore and Nachmias (1971) but much narrower than the 45 deg reported by Greenlee and Magnussen (1988). The discrepancies may have resulted from differences in task, stimulus characteristics (Phillips & Wilson, 1984), or both. In this study, we varied the orientation bandwidth of external noise rather than the test orientation. An important feature of our study is that we were able to separate the bandwidth of the signal path and the gain-control path.

In the cgcPTM, the bandwidth of the perceptual template in the signal path is much narrower than that in the gain-control path; the change of the gains of the perceptual template in both the signal and the gain-control paths is limited to a narrow orientation bandwidth. This suggests that, after adaptation, the observer is more sensitive to stimuli outside the adapted channel. This prediction is consistent with the observation that beyond one to three octaves of the adapted spatial frequency, adaptation may facilitate grating detection (De Valois, 1977; Tolhurst & Barfield, 1978).

We have developed the cgcPTM and used it to model effects of adaptation on detecting gratings embedded in external noise. A relatively high-contrast adapting grating and a brief target grating were used. The external noise paradigm produced highly informative data with strong constraints on observer models. We found that adaptation reduced the contrast gain to the adapted stimulus. As a result, it shifted psychometric functions to the right without changing their slopes. Such slope-invariant rightward shift of psychometric functions would make the visual system more sensitive to higher contrast stimuli, consistent with the notion that contrast-gain control may be the visual system's way to self-calibrate (Greenlee et al., 1991; Greenlee & Heitger, 1988).

Appendix A

The PTM (Lu & Dosher, 1999) was proposed to explicitly model nonlinear psychometric functions (Pelli, 1985) and the Weber law behavior of the perceptual system (Burgess & Colborne, 1988). Following traditions in pattern vision (Foley & Legge, 1981) and in observer modeling (Burgess & Colborne, 1988, Eckstein, Ahumada, & Watson, 1997), the PTM includes a nonlinear transducer function and a form of multiplicative noise to account for the nonlinear properties in perception. However, contrast-gain control rather than multiplicative noise is a more familiar model construct in the neurophysiology literature (e.g., Heeger, 1993). In this appendix, we develop a contrast-gain-control version of the PTM and show that the cgcPTM is mathematically equivalent to the original PTM.

The cgcPTM

As shown in Figure A1, the cgcPTM consists of six elements: (1) a perceptual template, (2) a nonlinear transducer function, (3) pre-gain-control internal noise, (4) contrast-gain control, (5) post-gain-control internal noise, and (6) a decision process. We describe each component in turn:

1. *The perceptual templates*. The perceptual template in the signal path passes input stimuli of specific spatial frequency and orientation through a processor with different gains. Prior to adaptation, we assume that the total gain across feature space and time equals 1.0 and that the gain for a signal-valued stimulus is equal to β. For a signal stimulus of contrast c, the perceptual template output has an amplitude S: $S = \beta c$. In the gain-control path, the perceptual template could be broader than that in the signal path. Again, without losing generality, we can set the total gain of the perceptual template as 1.0 and its gain to the signal stimulus to β_2. In addition to the signal is external noise (white Gaussian noise added by the experimenter) with equal energy across all spatial frequencies. Because its total gain is equal to 1.0, the perceptual template's output for external noise has a standard deviation σ_{ext} that is equal to the standard deviation N_{ext} of the external noise.
2. *The nonlinear transducer function* $y = x^{\gamma}$ processes the signal and external noise such that $S' = \beta^{\gamma} c^{\gamma}$ and $\sigma'_{\text{ext}} = N^{\gamma}_{\text{ext}}$.
3. *Pre-gain-control internal noise* is an internal noise source after the nonlinear transducer. It is modeled with a Gaussian distribution of mean 0 and standard deviation N_1. At this point, the noise in the system σ is characterized by both the external noise and the additive internal noise such that

$$\sigma^2 = \sigma^2_{\text{ext}} + \sigma^2_1 = N^{2\gamma}_{\text{ext}} + N^2_1,$$

and the net energy E in the gain-control path is

$$E = \beta_2^{2\gamma} c^{2\gamma} + N^{2\gamma}_{\text{ext}} + N^2_1.$$

4. A divisive *contrast-gain-control* process modifies the stimulus gain such that[2]:

$$S'' = \frac{\beta^{\gamma} c^{\gamma}}{\sqrt{b + E}}.$$

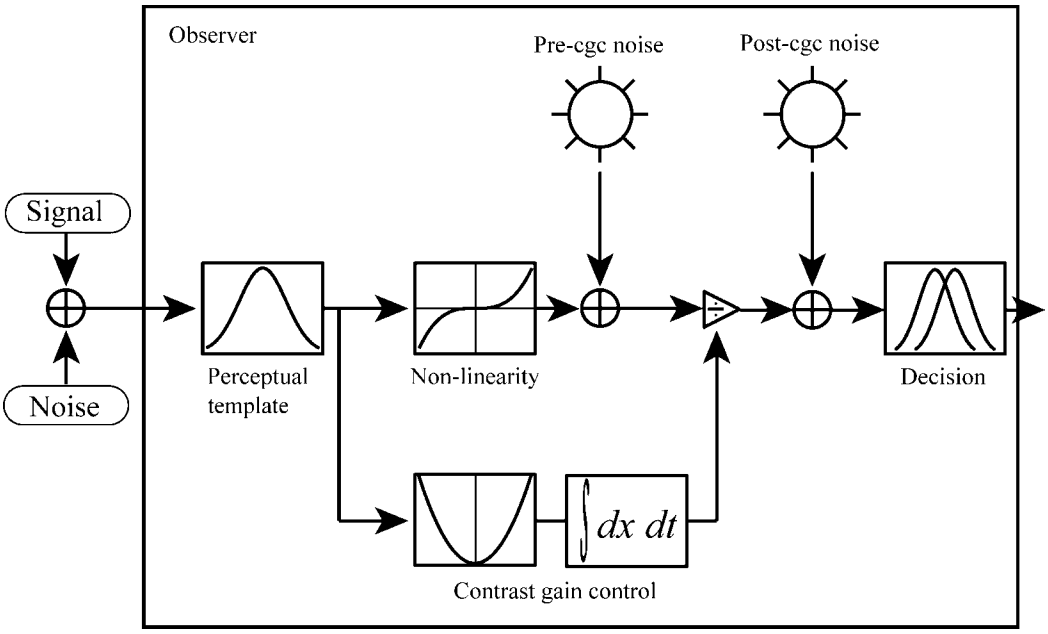

Figure A1. The cgcPTM.

Similarly, the noise variance is divided by stimulus energy:

$$\sigma'^2 = \frac{N_{\text{ext}}^{2\gamma} + N_1^2}{b + E}.$$

5. A second *post-gain-control* internal noise follows after contrast-gain control has been implemented and is modeled as a Gaussian random variable with mean 0 and standard deviation N_2. Therefore, the variance of all the noise sources is equal to the sum of the variances of all the noises:

$$\sigma_{\text{total}}^2 = \frac{N_{\text{ext}}^{2\gamma} + N_1^2}{b + E} + N_2^2.$$

6. At the *decision stage*, the signal and all the noises are combined. The details of the decision process depend on the particular task, for example, detection versus identification. These are modeled elsewhere (Macmillan & Creelman, 1991). Here, we focus on signal–noise discriminability, d', expressed as the signal-to-noise ratio:

$$d' = \frac{S''}{\sigma_{\text{total}}} = \frac{\beta^\gamma c^\gamma / \sqrt{b+E}}{\sqrt{\left(N_{\text{ext}}^{2\gamma} + N_1^2\right)/(b+E) + N_2^2}} = \frac{\beta^\gamma c^\gamma}{\sqrt{N_{\text{ext}}^{2\gamma} + N_2^2\left(\beta_2^{2\gamma} c^{2\gamma} + N_{\text{ext}}^{2\gamma}\right) + \left[N_1^2 + N_2^2(b+N_1^2)\right]}}. \quad \text{(A1)}$$

For the two-interval forced-choice task used in this study, the probability of a correct response is:

$$P_C = \int_{-\infty}^{+\infty} g\left(x - d', 0, 1\right) G(x, 0, 1)\mathrm{d}x, \quad \text{(A2)}$$

where $g(x,\mu,\sigma)$ and $G(x,\mu,\sigma)$ are the probability density and cumulative density functions of a Gaussian distribution, respectively.

For a given criterion d' level, we can solve the above equation to obtain the threshold contrast c_τ:

$$c_\tau = \left[\frac{N_{\text{ext}}^{2\gamma}\left(1 + N_2^2\right) + \left[N_1^2 + N_2^2\left(b + N_1^2\right)\right]}{\beta^{2\gamma}/d'^2 - N_2^2\beta_2^{2\gamma}}\right]^{\frac{1}{2\gamma}}. \quad \text{(A3)}$$

The cgcPTM and PTM equivalency

The cgcPTM and the original PTM (Figure A2) have rather different information-processing architectures. In the cgcPTM, the contrast-gain-control mechanism modifies the signal and noise via a divisive nonlinearity; there are two "fixed" noise sources, one pre- and the other post-gain control. The original PTM, on the other hand, has no such gain-control mechanism. It postulates two internal noise sources, one with fixed variance, and the other, multiplicative noise, with its variance proportional to the total energy in the stimulus as measured by the perceptual system. Here, we show that, despite the differences in

processing architecture, the two models produce mathematically equivalent functional input–output relationship between d' and the physical description of the input stimuli, that is, signal contrast c and external noise contrast N_{ext}.

A diagram of the original PTM (Lu & Dosher, 1999) is shown in Figure A2. The model describes signal–noise discriminability d' as:

$$d' = \frac{\beta^{\gamma} c^{\gamma}}{\sqrt{N_{ext}^{2\gamma} + N_{mul}^{2}\left(\beta_2^{2\gamma} c^{2\gamma} + N_{ext}^{2\gamma}\right) + N_{add}^{2}}}, \quad \text{(A4)}$$

where N_{add} is the standard deviation of the additive noise, N_{mul} is the proportional constant for multiplicative noise, and the rest of the symbols, d', β, β_2, c, and N_{ext}, are the same as their counterparts in cgcPTM.

It is obvious that Equations A1 and A4 are functional equivalent because the coefficients of external variables, c and N_{ext}, can be remapped into each other:

$$\begin{cases} N_{mul} = N_2 \\ N_{add} = \sqrt{N_1^2 + N_2^2\left(b + N_1^2\right)} \end{cases}. \quad \text{(A5)}$$

In other words, for any (N_1, N_2, b) parameterization of the cgcPTM, one can produce an equivalent (N_{add}, N_{mul}) parameterization of the original PTM such that the two models make equivalent predictions of d' as a function of c and N_{ext}. Conversely, in other words, for any (N_{add}, N_{mul}) parameterization of the original PTM, one can produce an equivalent (N_1, N_2, b) parameterization of the cgcPTM such that the two models make equivalent predictions of d' as a function of c and N_{ext}.

Modeling effects of adaptation

Adaptation may change a number of parameters in the cgcPTM. To determine which factors were altered following adaptation, we constructed a model lattice to look for the most parsimonious model that accounted for the data. Several factors were considered. Adaptation may (1) reduce the gain to signal stimuli from β to $u_1\beta$ in the signal path and from β_2 to $u_1\beta_2$ in the contrast-gain-control path, (2) reduce the gain to external noise from 1.0 to u_2, (3) alter the exponent of the nonlinear transducer function from γ to γ', (4) change N_1 to N_1', and/or (5) change N_2 to N_2'.

In the fullest model, we postulated that adaptation caused all the possible changes in the cgcPTM. Whereas Equation A2 expresses d' as a function of input stimuli and the model parameters prior to adaptation, after adaptation, the d' equation becomes:

$$d' = \frac{(u_1\beta)^{\gamma'} c^{\gamma'}}{\sqrt{Total\ Variance}};$$

$$Total\ Variance = (u_2 N_{ext})^{2\gamma'} + N_2'^2\left[(u_1\beta_2)^{2\gamma'} c^{2\gamma'} + (u_2 N_{ext})^{2\gamma'}\right] + \left[N_1'^2 + N_2'^2\left(b + N_1'^2\right)\right]. \quad \text{(A6)}$$

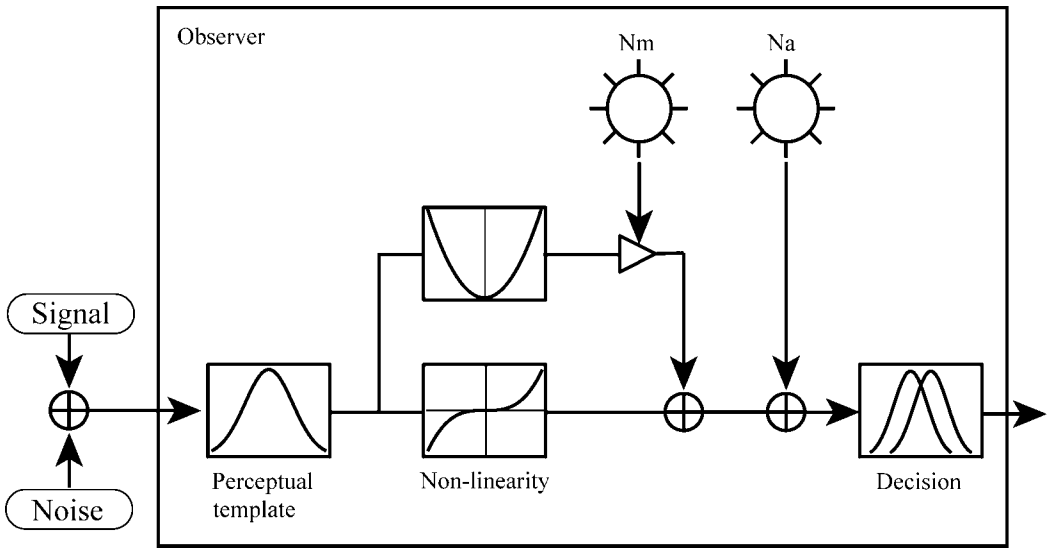

Figure A2. The PTM.

Correspondingly, contrast thresholds are expressed as:

$$c_\tau = \left[\frac{(u_2 N_{\text{ext}})^{2\gamma'}\left(1 + N_2'^2\right) + \left[N_1'^2 + N_2'^2\left(b + N_1'^2\right)\right]}{(u_1\beta)^{2\gamma'}/d'^2 - N_2'^2(u_1\beta_2)^{2\gamma'}}\right]^{\frac{1}{2\gamma'}}. \quad \text{(A7)}$$

Therefore, the fullest model (Model 1) had $k = 10$ parameters.[3]

The full model lattice consisted of 32 different combinations of all the possible adaptation effects. Only the six most meaningful reduced models were considered in addition to the fullest model. In Model 2 ($k = 7$), adaptation only affected internal noises: $N_1 \rightarrow N_1'$ and $N_2 \rightarrow N_2'$. In Model 3 ($k = 7$), adaptation reduced the gain to signal ($\beta \rightarrow u_1\beta$, $\beta_2 \rightarrow u_1\beta_2$) and external noise ($N_{\text{ext}} \rightarrow u_2 N_{\text{ext}}$). In Model 4 ($k = 6$), adaptation only changed the exponent of the nonlinear transducer: $\gamma \rightarrow \gamma'$. In Model 5 ($k = 6$), adaptation only impacted the gain to signal stimuli: $\beta \rightarrow u_1\beta$ and $\beta_2 \rightarrow u_1\beta_2$. In Model 6 ($k = 6$), adaptation only impacted the gain external noise: $N_{\text{ext}} \rightarrow u_2 N_{\text{ext}}$. Lastly, in the most reduced model (Model 7; $k = 5$), adaptation had no impact on any of the components of the cgcPTM.

Appendix B

The cgcPTM can be used to infer the shape and orientation tuning of the perceptual template. We inferred the shape of the perceptual template through the impact of noise and cgcPTM modeling. In this study, we orientation filtered the external noise about the adapted orientation—45 ± θ deg; all external noise conditions were presented at 100% contrast. In theory, the impact of external noise at 45 deg should be greatest because the noise is at the signal orientation. As we increase the bandwidth about 45 deg, the impact of increased external noise should be reduced (Figure B1). The gain on external noise at each noise bandwidth can be used to infer the perceptual templates' shapes.

We estimated the gain at each external noise bandwidth by assuming a Gaussian shape for the perceptual templates in both the signal path and the contrast-gain-control path of the cgcPTM:

$$T_{\text{signal path}}(\Delta\theta) = \frac{1}{\pi^{1/4}\sigma_1^{1/2}} e^{-\frac{(\Delta\theta)^2}{2\sigma_1^2}}, \quad \text{(B1)}$$

$$T_{\text{gain-control path}}(\Delta\theta) = \frac{1}{\pi^{1/4}\sigma_2^{1/2}} e^{-\frac{(\Delta\theta)^2}{2\sigma_2^2}}. \quad \text{(B2)}$$

In this framework, the standard deviations σ_1 and σ_2 of the two Gaussian-shaped templates were estimated as free parameters, and the gain at each external noise bandwidth was extrapolated from these templates.

Following adaptation, the perceptual templates in the signal and contrast-gain-control path were reduced at the adapted orientation by a notch, modeled by subtracting a third Gaussian shape with an estimated standard deviation σ_3. The amplitude of the notch is proportional to the

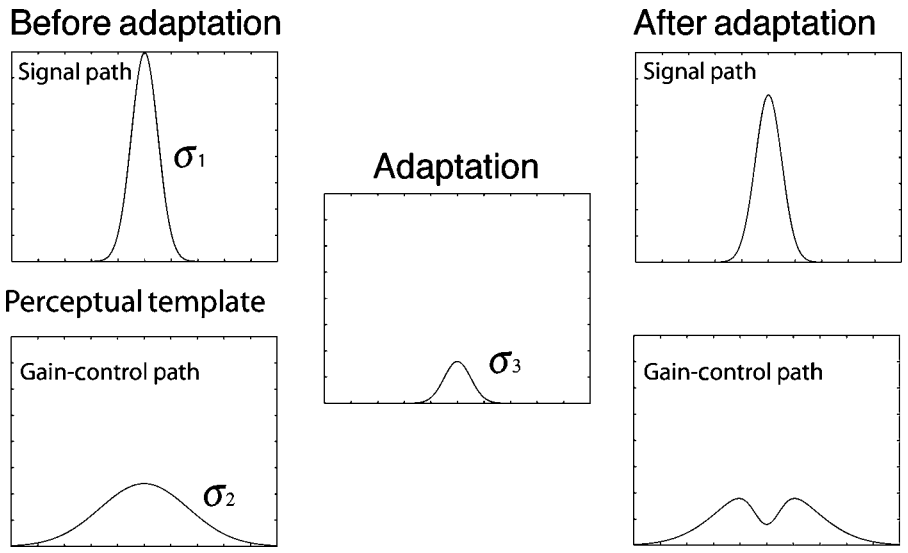

Figure B1. Perceptual templates before and after adaptation. Before adaptation, the templates in signal and gain-control paths are both modeled as Gaussian functions. The impact of adaptation is modeled as notches on the perceptual templates.

maximum amplitude of the corresponding template prior to adaptation. Therefore,

$$T'_{\text{signal path}}(\Delta\theta) = T_{\text{signal path}}(\Delta\theta) - \frac{k_3}{\pi^{1/4}\sigma_1^{1/2}} e^{-\frac{(\Delta\theta)^2}{2\sigma_3^2}}, \quad \text{(B3)}$$

$$T'_{\text{gain-control path}}(\Delta\theta) = T_{\text{gain-control path}}(\Delta\theta) - \frac{k_3}{\pi^{1/4}\sigma_2^{1/2}} e^{-\frac{(\Delta\theta)^2}{2\sigma_3^2}}. \quad \text{(B4)}$$

For each external noise bandwidth $\Delta\theta_i$, the variance of external noise following each perceptual template matching is then calculated by integrating the gain of the corresponding perceptual template from $-\Delta\theta_i$ to $\Delta\theta_i$:

$$\text{Var} = \int_{-\Delta\theta_i}^{\Delta\theta_i} T^2(\Delta\theta) d(\Delta\theta). \quad \text{(B5)}$$

The threshold contrasts at each external noise bandwidth were then estimated using Equation A7 with the estimated gain on external noise. Template standard deviations, pre-gain-control internal noise, post-gain-control internal noise, nonlinear transducer, and signal gain were estimated as free parameters.

Acknowledgment

This research was supported by NSF grants BCS-9911801 and BCS-9910678 and NIMH grant R01 MH61834-01.

Commercial relationships: none.
Corresponding author: Zhong-Lin Lu.
Email: zhonglin@usc.edu.
Address: Department of Psychology, SGM 501, 3620 McClintock Avenue, University of Southern California, Los Angeles, CA 90089-1061, USA.

Footnotes

[1]The term "TvC functions" has been used to describe threshold versus pedestal contrast functions in pedestal-masking studies. The same term has also been used to describe threshold versus external noise contrast functions in external noise studies. Please refer to the context when interpreting the term.

[2]In the formulation of a divisive contrast-gain-control model, the threshold "b" is required to regulate the model; that is, the response of the gain-control unit does not go to zero when the signal and external noise contrasts are near zero.

[3]In modeling TvC functions, we have generally assumed $\beta_2 = \beta$ because letting β_2 free to vary does not improve model fits. However, β_2 is critical in experiments that measure the shape of the perceptual template (e.g., Experiment 2).

References

Ahumada, A. J., Jr., & Watson, A. B. (1985). Equivalent-noise model for contrast detection and discrimination. *Journal of the Optical Society of America A, Optics and Image Science, 2,* 1133–1139. [PubMed]

Barlow, H. B. (1956). Retinal noise and absolute threshold. *Journal of the Optical Society of America, 46,* 634–639. [PubMed]

Barlow, H. B. (1990). A theory about the functional role and synaptic mechanism of visual aftereffects. In C. Blakemore (Ed.), *Vision: Coding and efficiency* (pp. 363–375). Cambridge: Cambridge University Press.

Barlow, H. B., MacLeod, D. I., & van Meeteren, A. (1976). Adaptation to gratings: No compensatory advantages found. *Vision Research, 16,* 1043–1045. [PubMed]

Blakemore, C., & Campbell, F. W. (1969a). Adaptation to spatial stimuli. *Journal of Physiology, 200,* 11P–13P. [PubMed]

Blakemore, C., & Campbell, F. W. (1969b). On the existence of neurones in the human visual system selectively sensitive to the orientation and size of retinal images. *The Journal of Physiology, 203,* 237–260. [PubMed] [Article]

Blakemore, C., Muncey, J. P., & Ridley, R. M. (1973). Stimulus specificity in the human visual system. *Vision Research, 13,* 1915–1931. [PubMed]

Blakemore, C., & Nachmias, J. (1971). The orientation specificity of two visual aftereffects. *The Journal of Physiology, 213,* 157–174. [PubMed] [Article]

Brainard, D. H. (1997). The Psychophysics Toolbox. *Spatial Vision, 10,* 433–436. [PubMed]

Burgess, A. E., & Colborne, B. (1988). Visual signal detection: IV. Observer inconsistency. *Journal of the Optical Society of America A, Optics and Image Science, 5,* 617–627. [PubMed]

Burgess, A. E., Wagner, R. F., Jennings, R. J., & Barlow, H. B. (1981). Efficiency of human visual signal discrimination. *Science, 214,* 93–94. [PubMed]

Carandini, M. (2000). Visual cortex: Fatigue and adaptation. *Current Biology, 10,* R605–R607. [PubMed] [Article]

Carandini, M., & Ferster, D. (1997). A tonic hyperpolarization underlying contrast adaptation in cat visual cortex. *Science, 276,* 949–952. [PubMed]

Crowder, N. A., Price, N. S., Heietanen, M. A., Dreher, B., Clifford, C. W., & Ibbotson, M. R. (2006). Relationship between contrast adaptation and orientation tuning in V1 and V2 of cat visual cortex. *Journal of Neurophysiology, 95,* 271–283. [PubMed]

De Valois, K. K. (1977). Spatial frequency adaptation can enhance contrast sensitivity. *Vision Research, 17,* 1057–1065. [PubMed]

Dean, A. F. (1983). Adaptation-induced alteration of the relation between response amplitude and contrast in cat striate cortical neurons. *Vision Research, 23,* 249–256. [PubMed]

DeBruyn, E. J., & Bonds, A. B. (1986). Contrast adaptation in cat visual cortex is not mediated by GABA. *Brain Research, 383,* 339–342. [PubMed]

Derrington, A. M., & Lennie, P. (1984). Spatial and temporal contrast sensitivities of neurons in lateral geniculate nucleus of macaque. *The Journal of Physiology, 357,* 219–240. [PubMed] [Article]

Dosher, B. A., & Lu, Z. L. (1998). Perceptual learning reflects external noise filtering and internal noise reduction through channel reweighting. *Proceedings of the National Academy of Sciences of the United States of America, 95,* 13988–13993. [PubMed] [Article]

Dosher, B. A., & Lu, Z. L. (2000). Mechanisms of perceptual attention in precuing of location. *Vision Research, 40,* 1269–1292. [PubMed]

Eckstein, M. P., Ahumada, A. J., Jr., & Watson, A. B. (1997). Visual signal detection in structured backgrounds: II. Effects of contrast gain control, background variations, and white noise. *Journal of the Optical Society of America A, Optics, Image Science, and Vision, 14,* 2406–2419. [PubMed]

Finlayson, P. G., & Cynader, M. S. (1995). Synaptic depression in visual cortex tissue slices: An in vitro model for cortical neuron adaptation. *Experimental Brain Research, 106,* 145–155. [PubMed]

Foley, J. M. (1994). Human luminance pattern-vision mechanisms: Masking experiments require a new model. *Journal of the Optical Society of America A, Optics, Image Science, and Vision, 11,* 1710–1719. [PubMed]

Foley, J. M., & Boynton, G. M. (1993). Forward pattern masking and adaptation: Effects of duration, interstimulus interval, contrast, and spatial and temporal frequency. *Vision Research, 33,* 959–980. [PubMed]

Foley, J. M., & Chen, C. C. (1997). Analysis of the effect of pattern adaptation on pattern pedestal effects: A two-process model. *Vision Research, 37,* 2779–2788. [PubMed]

Foley, J. M., & Legge, G. E. (1981). Contrast detection and near-threshold discrimination in human vision. *Vision Research, 21,* 1041–1053. [PubMed]

Gardner, J. L., Sun, P., Waggoner, R. A., Ueno, K., Tanaka, K., & Cheng, K. (2005). Contrast adaptation and representation in human early visual cortex. *Neuron, 47,* 607–620. [PubMed] [Article]

Georgeson, M. A., & Harris, M. G. (1984). Spatial selectivity of contrast adaptation: Models and data. *Vision Research, 24,* 729–741. [PubMed]

Green, D. M. (1990). Stimulus selection in adaptive psychophysical procedures. *Journal of the Acoustical Society of America, 87,* 2662–2674. [PubMed]

Greenlee, M. W., Georgeson, M. A., Magnussen, S., & Harris, J. P. (1991). The time course of adaptation to spatial contrast. *Vision Research, 31,* 223–236. [PubMed]

Greenlee, M. W., & Heitger, F. (1988). The functional role of contrast adaptation. *Vision Research, 28,* 791–797. [PubMed]

Greenlee, M. W., & Magnussen, S. (1988). Interactions among spatial frequency and orientation channels adapted concurrently. *Vision Research, 28,* 1303–1310. [PubMed]

Greenlee, M. W., & Thomas, J. P. (1992). Effect of pattern adaptation on spatial frequency discrimination. *Journal of the Optical Society of America A, Optics and Image Science, 9,* 857–862. [PubMed]

Hammett, S. T., & Snowden, R. J. (1995). The effect of contrast adaptation on briefly presented stimuli. *Vision Research, 35,* 1721–1725. [PubMed]

Hammett, S. T., Snowden, R. J., & Smith, A. T. (1994). Perceived contrast as a function of adaptation duration. *Vision Research, 34,* 31–40. [PubMed]

Hays, W. L. (1988). *Statistics* (4th ed., pp. xix, 1029). Fort Worth, TX: Holt, Rinehart, & Winston.

Heeger, D. J. (1993). Modeling simple-cell direction selectivity with normalized, half-squared, linear operators. *Journal of Neurophysiology, 70,* 1885–1898. [PubMed]

Jones, R. M., & Tulunay-Keesey, U. (1980). Phase selectivity of spatial frequency channels. *Journal of the Optical Society of America, 70,* 66–70. [PubMed]

Li, X., Lu, Z. L., Xu, P., Jin, J., & Zhou, Y. (2003). Generating high gray-level resolution monochrome displays with conventional computer graphics cards and color monitors. *Journal of Neuroscience Methods, 130,* 9–18. [PubMed]

Lu, Z. L., & Dosher, B. A. (1998). External noise distinguishes attention mechanisms. *Vision Research, 38,* 1183–1198. [PubMed]

Lu, Z. L., & Dosher, B. A. (1999). Characterizing human perceptual inefficiencies with equivalent internal noise. *Journal of the Optical Society of America A, Optics and Image Science, 16,* 764–778. [PubMed]

Lu, Z. L., & Sperling, G. (1995). Attention-generated apparent motion. *Nature, 377,* 237–239. [PubMed]

Macmillan, N. A., & Creelman, C. D. (1991). *Detection theory: A user's guide* (pp. xv, 407). New York, NY: Cambridge University Press.

Mafei, L., Fiorentini, A., & Bisti, S. (1973). Neural correlate of perceptual adaptation to gratings. *Science, 182,* 1036–1038. [PubMed]

Magnussen, S., & Greenlee, M. W. (1985). Marathon adaptation to spatial contrast: Saturation in sight. *Vision Research, 25,* 1409–1411. [PubMed]

Mather, G., Verstraten, F., & Anstis, S. (1998). *The motion aftereffects*. Cambridge, MA: MIT Press.

McLean, J., & Palmer, L. A. (1996). Contrast adaptation and excitatory amino acid receptors in cat striate cortex. *Visual Neuroscience, 13,* 1069–1087. [PubMed]

Meese, T. S., & Holmes, D. J. (2002). Adaptation and gain pool summation: Alternative models and masking data. *Vision Research, 42,* 1113–1125. [PubMed]

Menees, S. M. (1998). The effect of spatial frequency adaptation on the latency of spatial contrast detection. *Vision Research, 38,* 3933–3942. [PubMed]

Movshon, J. A., & Lennie, P. (1979). Pattern selective adaptation in cortical neurones. *Nature, 278,* 850–852. [PubMed]

Nagaraja, N. S. (1964). Effect of luminance noise on contrast thresholds. *Journal of the Optical Society of America, 54,* 950–955.

Ohzawa, I., Sclar, G., & Freeman, R. D. (1985). Contrast gain control in the cat's visual system. *Journal of Neurophysiology, 45,* 651–667. [PubMed]

Pantle, A., & Sekuler, R. (1968). Size-detecting mechanisms in human vision. *Science, 162,* 1146–1148. [PubMed]

Pelli, D. G. (1981). *Effects of visual noise*. PhD dissertation, University of Cambridge, Cambridge, England.

Pelli, D. G. (1985). Uncertainty explains many aspects of visual contrast detection and discrimination. *Journal of the Optical Society of America A, Optics and Image Science, 2,* 1508–1532. [PubMed]

Pelli, D. G. (1997). The VideoToolbox software for visual psychophysics: Transforming numbers into movies. *Spatial Vision, 10,* 437–442. [PubMed]

Pelli, D. G., & Zhang, L. (1991). Accurate control of contrast on microcomputer displays. *Vision Research, 31,* 1337–1350. [PubMed]

Phillips, G. C., & Wilson, H. R. (1984). Orientation bandwidths of spatial mechanisms measured by masking. *Journal of the Optical Society of America A, Optics and Image Science, 1,* 226–232. [PubMed]

Ross, J., Speed, H. D., & Morgan, M. J. (1993). The effects of adaptation and masking on incremental thresholds for contrast. *Vision Research, 33,* 2051–2056. [PubMed]

Sanches-Vives, M. V., Nowak, L. G., & McCormick, D. A. (2000a). Cellular mechanisms of long-lasting adaptation in visual cortical neurons in vitro. *Journal of Neuroscience, 20,* 4286–4299. [PubMed] [Article]

Sanches-Vives, M. V., Nowak, L. G., & McCormick, D. A. (2000b). Membrane mechanisms underlying contrast adaptation in cat area 17 in vivo. *Journal of Neuroscience, 20,* 4267–4285. [PubMed] [Article]

Sclar, G., Lennie, P., & DePriest, D. D. (1989). Contrast adaptation in striate cortex of macaque. *Vision Research, 29,* 747–755. [PubMed]

Shapley, R., & Enroth-Cugell, C. (1984). Visual adaptation and retinal gain controls. *Progress in Retinal Research, 3,* 263–343.

Sharpe, C. R., & Tolhurst, D. J. (1973). Orientation and spatial frequency channels in peripheral vision. *Vision Research, 13,* 2103–2112. [PubMed]

Snowden, R. J., & Hammett, S. T. (1996). Spatial frequency adaptation: Threshold elevation and perceived contrast. *Vision Research, 36,* 1797–1809. [PubMed]

Solomon, S. G., Peirce, J. W., Dhruv, N. T., & Lennie, P. (2004). Profound contrast adaptation early in the visual pathway. *Neuron, 42,* 155–162. [PubMed] [Article]

Stecher, S., Sigel, C., & Lange, R. V. (1973a). Composite adaptation and spatial frequency interactions. *Vision Research, 13,* 2527–2531. [PubMed]

Stecher, S., Sigel, C., & Lange, R. V. (1973b). Spatial frequency channels in human vision and the threshold for adaptation. *Vision Research, 13,* 1691–1700. [PubMed]

Stromeyer, C. F., III, Klein, S., Dawson, B. M., & Spillmann, L. (1982). Low spatial-frequency channels in human vision: Adaptation and masking. *Vision Research, 22,* 225–233. [PubMed]

Stromeyer, C. F., III, Klein, S., & Sternheim, C. E. (1977). Is spatial adaptation caused by prolonged inhibition? *Vision Research, 17,* 603–606. [PubMed]

Tolhurst, D. J., & Barfield, L. P. (1978). Interactions between spatial frequency channels. *Vision Research, 18,* 951–958. [PubMed]

Wainwright, M. J. (1999). Visual adaptation as optimal information transmission. *Vision Research, 39,* 3960–3974. [PubMed]

Williams, D. W., Wilson, H. R., & Cowan, J. D. (1982). Localized effects of spatial frequency adaptation. *Journal of the Optical Society of America, 72,* 878–887. [PubMed]

Wilson, H. R., & Humanski, R. (1993). Spatial frequency adaptation and contrast gain control. *Vision Research, 33,* 1133–1149. [PubMed]